Geometric and Material Effects on Bamboo Buckling Behaviour

Kent A. Harries[1], James Bumstead[2], Michael Richard[3] and David Trujillo[4]

Abstract

Bamboo is a functionally graded material that has evolved to resist its primary loading in nature. This study focuses on the effects of geometric and material property variation along the culm length on the capacity of an axially-loaded member. Conservatively, compression capacity may be calculated using the smallest section of the member; however, this results in an inefficient use of the culm and may limit the use of long compression members. A more realistic estimate of capacity is obtained by considering the effects of culm taper on buckling capacity. Culm taper is experimentally investigated for three representative bamboo species. The effects of culm section gradient on geometric properties is examined followed by an assessment of geometric variation along the culm height. Following this, a series of buckling analyses of tapered culms is conducted to illustrate the significant effects of taper on culm compression capacity. This analysis is supplemented with comparisons to experimental culm buckling data. Beyond compressive capacity, the implications of culm taper are discussed in terms of flexural behaviour, design of gridshells (involving pre-bent axial load-carrying members), visual grading of bamboo and ultimately classification of the many species of bamboo presently used in construction worldwide.

Keywords: Columns, Developing Countries, Materials Technology

[1] Bicentennial Board of Visitors Faculty Fellow and Associate Professor, University of Pittsburgh, Department of Civil and Environmental Engineering, Pittsburgh, USA; kharries@pitt.edu
[2] Undergraduate Research Assistant, University of Pittsburgh, Department of Civil and Environmental Engineering
[3] Engineer, SGH, Boston; formerly PhD Researcher, University of Pittsburgh
[4] Senior Lecturer, Coventry University, Faculty of Engineering and Computing, Coventry, UK

Introduction

The structure of bamboo is composed of culms (poles) with solid transverse diaphragms or 'nodes' separating hollow inter-nodal regions along its height (Fig. 1a). The circular cross section (Figs 1b-d) is composed of unidirectional cellulosic fibers (about 40% by volume) oriented parallel to the culm's longitudinal axis embedded in a parenchyma tissue matrix (50%; the remaining 10% being vessels for fluid transport) (Janssen 2000). The parenchyma tissue matrix hardens or lignifies as the culm matures leading to an increase in density and an improvement in mechanical properties. Lignin content in bamboo is about 20 to 26%, similar to that of soft (24-37%) and hard (17-30%) wood species (Li et al. 2007).

Bamboo is a functionally graded material (FGM) that has evolved to resist its primary loading in nature: its own self-weight and the lateral effects of wind. As seen in Fig. 1c, the density of fibers increases from the culm's inner wall to the outer wall. The wall thickness is largest at the base of the culm and decrease with height up the culm. However, the size and quantity of vessels decrease with the height of the culm (used for nutrient transport, their volume may be reduced with increased culm height) and are replaced with cellulosic fibers. This addition of fibers compensates for loss in strength and stiffness due to reductions in diameter and wall thickness near the top of the culm, resulting in relatively uniform engineering properties along the entire culm height (Amada et al. 1996). Finally, the thin, dense, silica-containing outer layer of the culm wall serves as protection for the plant but can dull tools when bamboo is used in construction.

Material properties of bamboo are mostly comparable to conventional hard wood timber. Like any fiber-reinforced material, mechanical properties are highly correlated to the proportion and distribution of fibers in the cross section. Mechanical properties are influenced by density, which depends on fiber content, fiber diameter, and cell wall thickness (Janssen 2000). The density of most bamboo is 600 – 800 kg/m^3 but depends on species, growing conditions, and position along the culm. Fibers are approximately 60-70% by weight of the culm. The volume fraction of fibers ranges from approximately 60% at the exterior face of the culm wall to 10-15% near the interior face (Fig. 1c). The variation in density through

the culm wall has been assumed by previous researchers to be linear (Duff 1941; Janssen 1981; Vaessen and Janssen 1997), quadratic (Ghavami et al. 2003), exponential (Nogata and Takahashi 1995; Dixon and Gibson 2014) or a power function (Habibi et al. 2015) and is known to be species-dependent (Amada et al. 1996 and 1997). Regardless, due to the complex variation of the fibers and vascular bundles, the variation of mechanical properties through the culm-wall thickness has been shown to be significant (Richard and Harries 2015) and to have the effect of increasing gross culm stiffness by about 10% as compared to a uniform distribution of the same volume of fibers (Janssen 2000). Density also increases along the height of a culm (Amada et al. 1996; Janssen 2000; Correal and Arbelaez 2010). Additionally, the variation of density through the culm wall thickness has also been observed to vary somewhat with height as the fiber content becomes greater at the outer wall surface and less at the inner (Ghavami et al. 2003).

Why is Variation of Culm Section Geometry with Length of Interest?

An understanding of the variation of culm geometry along culm length may be relevant to the following areas or study.

Compression Behaviour **–** Bamboo culms are used as both columns and compression elements in truss structures. Due to their internode geometry, culm wall buckling is unlikely and most compression elements will have their capacity controlled by their global, or Euler buckling behaviour. Conservatively, this capacity may be calculated using the smallest section of the element; however, this results in an inefficient use of the culm and may limit the use of long compression members. A more realistic estimate of capacity is obtained by considering the effects of taper (Gere and Carter 1962; Williams and Aston, 1989) on culm buckling capacity (Yu et al. 2003).

Flexural Behaviour – Flexural tests are often used to assess suitability of bamboo culms for use in structural applications and to obtain values used in design including modulus of rupture (ISO 2004) and longitudinal shear capacity (Richard 2013). A tapered flexural element has a varying distribution of stress along the span affecting the determination of these fundamental properties (Naresworo and Bahtiar 2013).

Gridshell Design – Bamboo gridshell structures have been proposed (Eells et al. 2013). Techniques for form-finding for gridshells (Douthe et al. 2006) are based on uniform properties along the lengths of the members of the gridshell. Accurate knowledge of the mechanical and geometric properties of individual elements is essential in form-finding grid shells, determining their boundary conditions, and locating foundation elements and determining the stresses these must carry. Therefore being able to model the variation of properties along the length of a culm is critical if bamboo gridshells are to be developed. Without this, every gridshell will be designed in an ad hoc fashion in which the final shape and boundary conditions are only known after the shell has been formed; this is not practical for a gridshell of any practical size.

Visual Grading of Bamboo – Development of a standardised method of grading full-culm bamboo for structural use has been proposed (Trujillo 2013). Easily measured geometric properties such as diameter and internode length may be related to culm wall thickness, and therefore be used to estimate geometric properties without resorting to more complex non-destructive techniques to obtain the wall thickness. The present authors contend that internode spacing, culm diameter and culm wall thickness are related in order to ensure that the culm wall does not buckle due to the effects of axial or lateral load. Indeed, establishing relationships for the along-culm variation would require only dimensions at the top or bottom of the culm to be known.

Classification of Structural Bamboo – Every species of bamboo has different geometric and physical characteristics. While a handful of species dominate structural applications based on their regional availability (*Phyllostachys edulis* (Moso) in China, *Bambusa stenostachya* (Tre Gai) and *Dendrocalamus giganteus* in South East Asia, and *Guadua angustifolia* (Guadua) in South America, for instance), it is estimated that as many as 100 species are suitable for load-bearing applications (Liese 1987). If standardisation of full-culm bamboo is a goal, it will be practically necessary to classify species in some manner relative to their structural characteristics. The National Building Code of India (2005), for instance, classifies 16 species of Indian bamboo into three groups based on flexural behaviour (modulus of rupture and flexural modulus of elasticity); this requires destructive testing of culms. Shigematsu

(1957) proposed grouping bamboo species by their geometric characteristics, proposing four groupings based on observed *D/t* ratios (where *D* is the culm diameter and *t* is the wall thickness). Shigematsu presents formulae for estimating *D, t* and *D/t* for 16 Japanese species of bamboo (including Moso) based on culm length normalised by internode number, offering a potentially useful approach of visual classification and grading. The present authors contend that classifying species as being either thin- or thick-walled is a first step to structural classifications; this will be explored further in the present work.

Measured and Calculated Culm Geometric Parameters of a Bamboo Culm

The following measured culm geometric properties and notation are used in this paper (Figure 2).

n – internode number (base of culm : $n = 1$)

L – overall length of culm

L_n – length of internode n

D_n – diameter (average of two measurements) at middle of internode n

D_0 – diameter at base of culm

t_n – wall thickness (average of four measurements) at middle of internode n

From these, the following calculated geometric properties are obtained:

area of culm section: $A_n = (\pi/4)\,[D_n^2 - (D_n - 2t_n)^2]$ [1]

moment of inertia of culm section: $I_n = (\pi/64)[D_n^4 - (D_n - 2t_n)^4]$ [2]

radius of gyration of culm section: $r_n = (I_n/A_n)^{1/2} = 0.25[D_n^2 + (D_n - 2t_n)^2]^{1/2}$ [3]

Material Properties through Culm Wall Thickness

Often bamboo is treated as a fibre-reinforced material in which the ‘rule of mixtures’ is used with the fiber volume fraction, *V*, and gradation through the culm wall to determine modulus (e.g.: Ghavami et al. 2003; Amada et al. 1996; Ghavami 2008; Li and Shen 2011; Dixon and Gibson 2014). As shown

schematically in Figure 2, the longitudinal fibre volume ratio at internode $V_n(t)$ is a function of wall thickness t. The fibre volume ratios at the inner and outer regions of the culm wall (Fig. 1c) have been shown to be relatively consistent across species approximately equal to $V_{inner} = 0.10$ and $V_{outer} = 0.60$ (e.g.: Janssen 1981 and 2000; Nogata and Takahashi 1995; Ghavami et al. 2003; Dixon and Gibson 2014).

The longitudinal modulus of elasticity, $E_n(t)$ is assumed to be a function of $V_n(t)$ and determined using the rule of mixtures:

$$E = VE_f + (1\text{-}V)E_m \qquad [4]$$

Janssen (1981, 2000) estimates the elastic modulus of a bamboo fibre to be $E_f = 35000$ MPa and the elastic modulus of lignin as $E_m = 1800$ MPa. These values will be adopted as the basis for the following discussion.

As is typical when describing functionally graded materials, the modulus through the culm wall thickness may be given by the following:

$$E(t) = (E_{outer} - E_{inner})(t/t_n)^k + E_{inner} \qquad [5]$$

In which E_{outer} and E_{inner} are the moduli determined at $t = t_n$ and $t = 0$, respectively (Figure 2). The exponent k describes the fibre volume distribution; for instance, $k = 1$ for a linear distribution and $k = 2$ for quadratic. Habibi et al. (2015) report a value of $k = 0.43$ for samples of *p. edulis* (Moso); Dixon and Gibson (2014) report values ranging from $k = 1.64$ to 2.11 dependent on the height along the Moso culm and Nogata and Takahashi (1995) propose $k \approx 2.2$, also for Moso. In order to reasonably bound the results reported in the literature, in this discussion values of k= 0.5, 1.0 and 2.0 will be considered.

The variation of fibre volume and therefore modulus results in the 'centroid' of the wall cross section, t_c (see Figure 2) as measured by axial stiffness, EA, to shift outward from the geometric centroid of the wall (i.e., $t_c = 0.5t_n$). This shift is a measure of the effect of the assumed variation when compared to the section properties averaged over the gross culm cross section. The location of the 'centroid' of the modulus distribution will also vary based on the ratio E_f/E_m.

Variation of Material Properties Along Length of Culm

Extant studies of material property variation along the height of the culm typically break the culm into thirds, reporting values for the bottom, middle and top third of the culm. Little definitive data is available since researchers report different methods of obtaining modulus and variation clearly differs from species to species (Kamruzzaman et al. 2008). Correal and Arbeldez report an increase in compressive modulus along 15 m lengths of *G. angustifolia* from 16.3 to 17.9 GPa (10% increase) but no similar increase in modulus obtained from bending tests of 5 m lengths of the 15 m culm (17.2 GPa at bottom, middle and top locations). Amada et al (1996), on the other hand, report an increase in tensile modulus of about 50% (from about 11.3 to 17.3 GPa) over 13 m lengths of Moso. Kamruzzaman et al. (2008) report increases in flexural modulus averaging 29% for four Bangladeshi species of bamboo.

Based on Eq. 4, the fibre volume fraction, V, of a section may also stand surrogate for modulus. Qi et al (2014) report an increase in fibre volume of about 8% over 10 m culms of *Neosinocalamus affinis* while Amada et al. (1996) report an increase of almost 100% (from V = 20 to 40%). The latter result would appear to explain the 50% increase in tension modulus reported. The increase in V will be greater than the corresponding increase in modulus (Eq. 4).

Amada et al (1996) and Ghavami et al. (2003) report changes in the fibre volume distribution through the culm wall with height. At higher locations in the culm, the fibre volume fraction increases at the outer culm wall and decreases at the inner culm wall. While Amada et al. report a significant change in total fibre volume fraction with height (above), Ghavami et al. reports a smaller increase in total fibre content – about 12% – over approximately 11 m culms of *D. giganteus*.

Culm Section Stiffness

Due to the variation in fibre content and therefore modulus through the culm wall thickness, the effective or apparent axial (EA) and flexural (EI) stiffnesses of the culm section also vary based on the assumed fibre distribution.

In order to calculate the culm stiffness accounting for variation of modulus through the section, the culm wall is divided into ten concentric rings (i = 1 to 10) having equal thickness $t_n/10$ (Figure 3) and the stiffness properties (EA and EI) of each are determined and summed as follows.

The outer diameter of each ring is D_i:

$$D_i = D_n - 2t_n + 2i(t_n/10) \quad [6]$$

The geometric properties of the individual rings are:

$$A_i = (\pi/4)[D_i^2 - D_{i-1}^2] \quad [7]$$

$$I_i = (\pi/64)[D_i^4 - D_{i-1}^4] \quad [8]$$

The effective culm properties accounting for the variation of through thickness properties are therefore found from:

$$I_{eff} = \sum E_i I_i / E_{avg} \quad [9]$$

$$r_{eff} = \sum (E_i I_i / A_i E_i)^{1/2} \quad [10]$$

In which E_i is calculated at the middle of each ring using Eq. 5 and E_{avg} is the average value E_i across the entire culm wall.

A brief parametric study describing the impact of material variation in the culm section is presented in Table 1. In all cases, V_{inner} = 0.10 and V_{outer} = 0.60 as reported in multiple studies (e.g.: Janssen 1981 and 2000; Nogata and Takahashi 1995; Ghavami et al. 2003; Dixon and Gibson 2014). The effective section properties are affected by the ratio E_f/E_m rather than the specific values of these parameters; here the cases E_f/E_m = 10, 19.4 and 30 are considered where E_f/E_m = 19.4 corresponds to that reported by Janssen (1981, 2000). Similarly, the nature of the culm – be it thick- or thin-walled – impacts the effective properties; the cases D_n/t_n = 4 and 10 are shown. Three distributions of modulus (Eq. 5) through the culm wall are considered: k = 0.5, 1 and 2. Finally, the effective section properties (Eqs 9 and 10) are compared to the

gross section properties (Eqs 2 and 3) in order to illustrate the impact of through culm wall material variation.

If a single value of E is used across an entire section, $I_{eff} = I_n$, $r_{eff} = r_n$ and $t_c/t_n = 0.50$. Thus it is clearly seen in Table 1 that the effect of material property variation is to increase the effective geometric properties of a section. This is the functional gradation that has evolved from the natural loading on the growing bamboo: lateral wind loads and self-weight of the culms. The increase in effective geometric properties is seen to be a function of both E_f/E_m and D_n/t_n. For thin-walled bamboo ($D_n/t_n = 10$), the increases in effective moment of inertia and radius of gyration are nominal (approximately 6 and 2%, respectively) regardless of E_f/E_m or assumed material variation, k. For thick-walled bamboo ($D_n/t_n = 4$), the increases are naturally greater and proportional to both E_f/E_m and k. Previously, Janssen (2000) reports an increase in flexural stiffness of approximately 10% due to through-wall property gradation; this value agrees relatively well with the calculations presented.

Geometric Variation over Length of Culm

Detailed geometric measurements of *P. edulis* (Moso), *G. angustifolia* (Guadua) and *B. stenostachya* (Tre Gai) culms have been obtained for a variety of studies conducted by the authors' research groups. Most culms were used for concentric compression tests, in which case they were selected for their overall straightness and having minimal defects; thus the culms selected are representative of those suitable for structural use. Generally, overall culm length was about 2600 mm (Moso and Tre Gai) or 3600 mm (Guadua) and each culm included from 9 to 18 nodes. Moso and Guadua are 'thin-walled' species having a D/t ratios that average approximately 10 over the length of culms considered. Tre Gai is a 'thick-wall' species in which D/t averages approximately 5.5 over the culm length considered.

Culm diameter, D_n, internode lengths, L_n, and initial out-of-straightness were obtained using an apparatus reported by Richard (2013). The wall thickness, t_n, was measured following testing when the culm was cut at each internode section. Section geometric properties: area, A_n, moment of inertia, I_n, and radius of gyration, r_n, were calculated using Equations 1 to 3.

In order to analyse the geometric variation across all culms, section properties were normalized with respect to the values at the base of the culm (i.e., typically the location of the largest value of diameter) denoted with a subscript "0". Furthermore, data is presented using the location along the culm length normalised by the base diameter, L/D_0. Table 2 summarises observed trends in measured (D/D_0 and t/t_0) and calculated (A/A_0, I/I_0 and r/r_0) geometric properties along the normalised culm length, L/D_0. In all cases an exponential fit in the form of $D/D_0 = e^{\alpha(L/D_0)}$ provides the 'best fit'; the corresponding R^2 values are also reported in Table 2. Figure 4 shows the normalised geometric properties for all three species.

Thin-walled species P. pubescens (Moso)

Data for Moso was obtained from culms having diameters ranging from 60 to 120 mm and wall thicknesses ranging from 6 to 17 mm. Diameter exhibited a noticeable taper resulting in a reduction in diameter of about 20% over a typical 2500 mm long culm. Wall thickness taper was also observed to be significant resulting in a decrease of wall thickness of 20-50% along the length of a 2500 mm culm. Combining these observations, significant reductions in area and moment of inertia of up to 60% and 75%, respectively, are observed over typical 2500 mm long culms. The combined effect of this variation results in a decrease in the radius of gyration along the length of the culm of approximately 10 – 20% over a 2500 mm culm length.

Thin-walled species G. angustifolia (Guadua)

Data for Guadua was obtained from culms having diameters ranging from 50 to 130 mm and wall thicknesses ranging from 4 to 19 mm. In general, the scatter of the measurements from the Guadua culms was greater than that of the other two species. Diameter exhibited taper resulting in a reduction in diameter of about 10% over a typical 3500 mm long culm. Wall thickness taper was observed to be significant and to vary significantly (as low as 5% and as great as 50%) from culm to culm. Combining these observations, reductions in area and moment of inertia of approximately 40% were observed over typical 3500 mm long culms. The combined effect of this variation results in a decrease in the radius of

gyration along the length of the culm of approximately 10% although due to the large variation in measurements obtained, a number of culms exhibited a marginal increase in the value of radius of gyration over their length.

Thick-walled species B. stenostachya (Tre Gai)

Data for Tre Gai was obtained from culms having diameters ranging from 65 to 95 mm and wall thicknesses ranging from 10 to 24 mm. Diameter variation over the culm length for this species was negligible (hence the low R^2 value); typically diameter varied less than 5% from the D_0 value. Wall thickness taper was, however, observed to be significant resulting in a decrease of wall thickness of 30-50% along the length of a 2500 mm culm. Combining these observations, reductions in area and moment of were not as significant as for the Moso but were apparent nonetheless. Over typical 2500 mm long culms, reductions in area and moment of inertia were approximately 30%. Of particular interest is that in combining these effects, an ***increase*** in radius of gyration along the length of the culm is indicated.

Effect of Geometric and Material Property Variation on Culm Buckling

In order to investigate the effect of geometric and material variation on culm buckling, a series of analyses of pin-supported (i.e., effective length factor, $K = 1.0$) culms subject to axial load was conducted. Because it is relatively easily programmed into a spreadsheet, an approach using successive approximations of the deflected shape of the tapered column (Timoshenko and Gere 1961 Art. 2.15) was used to determine the critical buckling load of representative bamboo culms. The procedure is summarised as follows:

1. Assume an approximate deflected shape; a linear approximation was initially assumed between each culm end and midheight.
2. Determine internal moments due to unit axial load applied to culm having assumed deflected shape.
3. Determine deflections of column having bending moment distribution determined in step 2.
4. Normalise the deflections and update the approximate deflected shape with normalised deflections.

5. Repeat steps 2 through 4 until difference between successive iterations is negligible.
6. The critical buckling load is the inverse of the unnormalised maximum deflection from the final iteration.

To facilitate integration and modelling both geometric and material property variation, the culm height is divided into 50 segments of equal length. Thus, from the point of view of analysis, the culm taper is modelled as 50 steps rather than a continuous taper. The 50-segment solution approach adopted was benchmarked for prismatic columns and columns having a linear taper (Timoshenko and Gere 1961) and found to overestimate the 'exact' solutions by less than 0.2% and 1%, respectively. This degree of precision was determined to be acceptable.

Representative pin-ended bamboo culms having an effective length KL = 2500 mm were considered. The base diameter was D_0 = 100 mm and base wall thickness was t_0 = 10 mm (representing Moso having D_0/t_o = 10); 25 mm (Tre Gai having D_0/t_o = 4) or 9 mm (Guadua having D_0/t_o = 11). Nominal sectional properties were used (Eqs. 1 and 2). The bamboo modulus used was 15080 MPa (using Eq. 4 with V = *0.4*, E_f = 35,000 MPa and E_m = 1800 MPa). Culm geometric taper was modelled as both linear and using the relationships presented in Table 2. Culm modulus variation was assumed to be linear. Table 3 summarises the eight cases considered.

The results of the analyses are shown in Table 4. Values are normalised against Case II as this is the most conservative estimate of culm buckling capacity and the one most likely to be used in the field – that calculated with the smallest sectional geometry (top of culm) and nominal modulus. Similarly, the critical stress is calculated using the smallest section area – that at the top of the culm. Due to the effect of taper, the location of the greatest lateral deflection ($h_{\Delta max}$) shifts from mid-height toward the smaller end of the culm in the Moso and Guadua analyses (Cases V to VIII). This shift is relatively small and is mitigated by the increase in modulus from the larger to smaller end of the culm (Cases VII and VIII). No such shift is seen in the relatively mildly tapered Tre Gai analyses (due to the discretisation of the culm, a resolution of only 0.02L is available for locating $h_{\Delta max}$).

It is clear from Table 4 that considerable reserve axial capacity may be achieved over that calculated conservatively assuming a prismatic column having the smallest culm dimension (Case II). Case VI, while complicated to calculate, represents the most realistic estimate of behaviour if one assumes no variation of modulus along the culm length. For each 10% in increase in modulus at the top of the culm relative to that at the base, the buckling capacity increases about 5% (Cases VII and VIII). Simply using the average geometric properties in a prismatic buckling analysis (Case III) may overestimate the behaviour determined based on taper (Cases V and VI).

Case III is perhaps the simplest prismatic analysis to apply in practice – simply averaging measured dimensions from the base and top of the culm. However, since culm taper is not linear, this approach may overestimate the axial capacity. Case IV, in which a prismatic analysis is used having section properties calculated at mid-height ($L/D_0 = 12.5$ in this case) from the equations presented in Table 2 and a uniform modulus appears to provide a reasonable lower bound approximation of Cases VI to VIII, without the complexity of conducting a buckling analysis of a tapered column.

The difference between the prismatic cases III and IV is best described by the location along the culm height of the average moment of inertia. In most cases, the moment of inertia at the midheight of the culm is less than the average of the base and top moments of inertia. This results in the top of the culm being proportionally more flexible and therefore 'contributing' more to the buckling behaviour. This behaviour is manifest in the small shift of $h_{\Delta max}$, described above. Figure 5 shows the normalized moments of inertia at midheight for the culms reported in the database. It is seen that in the majority of cases, the average moment of inertia occurs closer to the base of the culm.

Comparison with Experimental Data

A summary of eight single culm buckling tests – four Moso specimens reported by Bumstead and Harries (2016) and four Tre Gai reported by Richard (2013) is presented in Table 5. The experimental buckling load is obtained from a Southwell (1932) analysis of experimental load versus lateral displacement. Analysis Cases are the same as those reported in Table 3 with the following exceptions: Case IV:

measured values of properties at mid-height are used; and, Case VI: the culm is discretised into its internodes (segments) and *measured* geometric properties are used; thus removing the averaging inherent in using the equations reported in Table 2. Only average experimentally determined modulus values are available, thus no modulus variation can be investigated (Cases VII and VIII).

The predictions are all consistent and conservative. Case VI may be considered the most realistic analysis as it accounts for the measured geometric taper in each culm. The buckling capacity predicted using Case VI is about 81% and 90% of the experimentally observed values for Moso and Tre Gai, respectively. Case IV predictions are similar: about 76% and 91% of the experimentally observed values for Moso and Tre Gai, respectively. The degree of conservativeness is perhaps appropriate in a design context. There are a number of factors hypothesized to contribute to the conservative nature of the predictions using Cases IV or VI:

1. The analyses do not account for the inherent stiffening effects described in Table 1.
2. As shown in Table 4, an increase in modulus with height along the culm has the effect of mitigating some of the taper effect. Each 10% increase in modulus has the effect of increasing the buckling load about 5%.
3. The end conditions in the experimental test set-up, while replicating pins, will necessarily have some restraint associated with them resulting in a marginally shorter effective length and therefore larger buckling load.
4. Experimental buckling tests are run in displacement control and, despite using the Southwell approach, are inherently ‘upper bound’ estimates of theoretical capacity.

Classification of Section Behaviour – Thin- vs. Thick-walled Culms

Considering the theoretical analyses and validations using experimental data presented, this study begins to suggest a method by which culms may be classified. Behaviour may be classified as being typical of thin- or thick-walled behaviour. Table 6 provides some general characteristics of each behaviour. It is proposed that the transition between behaviours be characterised by the variation of radius of gyration

since this captures both axial (A) and flexural (I) geometric properties. Figure 6 shows the data presented in the present study. Using an increase (thick-walled) or decrease (thin-walled) of the radius of gyration, r, with culm height as a metric, an easily measured D/t threshold of eight appears to divide the behaviours. Thus as an initial proposal, bamboo having $D/t > 8$ have the characteristics of a thin-wall species and those having $D/t < 8$ have the characteristics of a thick-walled species.

Discussion and Conclusions

Returning to the question *why is variation of culm section geometry with length of interest?,* this paper has illustrated a number of effects of the variation of bamboo properties and provided some basis for exploring others.

Classification of Structural Bamboo – As described in the previous section, an initial classification of thin- or thick-walled species helps to describe both geometric properties of culm cross sections and variation of properties along a culm. It is proposed that $D/t = 8$ is an appropriate threshold above which to classify behaviour as being thin-walled and below which behaviour is thick-walled. Clearly, extending the methodology presented in the present work to other species will permit this classification to be refined.

Compression Behaviour – It is shown that variation of bamboo properties both in a cross section and along the culm length result in improvement of compressive capacity over that which may be assumed in a simple analysis. The functionally-graded nature of bamboo in cross section has the effect of increasing the effective moment of inertia and radius of gyration above that calculated using section geometry alone. This effect is more pronounced in thick-wall sections in which the apparent moment of inertia may exceed 1.20 times that calculated using section geometry alone. For thinner-wall members, an increase of only about 1.05 is observed. Thus, while Janssen's rule-of-thumb of a 10% increase is generally valid, this may be better quantified as a 20% increase for thick-walled members and a 5% increase for thin-walled members.

Longitudinal variation of culm geometry (taper) also affects compressive behaviour. While calculating the bucking capacity of a tapered member is not practical in most instances, simply assuming prismatic member geometry having the smallest cross section (Case II in Tables 3 and 4) is overly conservative and may result in an inefficient use of the culm and/or limit the use of long compression members. This is especially the case for thin-walled members in which the actual buckling capacity may by 50% or more greater than this conservative estimate. However, due to the nature of the tapered geometric properties of the culm it may be nonconservative to simply take an average value of section properties (Case III) to assess buckling. The data presented indicates that buckling analysis of a prismatic member using measured mid-height properties (Case IV) provides an appropriate estimate of capacity without the complexity of analysing a tapered member. Neglecting the increase in effective section properties resulting from the functionally-graded nature of bamboo should result in sufficient confidence in such an estimate.

While there is very little data available to quantify the variation of modulus of elasticity with height along a culm, it is shown that this variation also results in increased buckling capacity. Assuming a linear variation of modulus, it is shown that for each 10% in increase in modulus at the top of the culm relative to that at the base, the buckling capacity increases about 5%.

Flexural Behaviour – The effect of the functionally graded nature of bamboo and the taper along the culm has not been adequately investigated with respect to flexural behaviour. Certainly the increase in effective section properties is relevant although, at this time, there is very little available data on the variation of shear properties with culm height (Correal and Arbeldez (2010) report no significant variation of shear strength with height for Guadua). The interaction of flexure and shear will also be affected by the geometry of the proposed flexural loading (i.e., the length of the shear span), making the discussion of flexural behaviour considerably more complex and a topic for significant further study.

Other Applications requiring full culm-height data – Having a better understanding of the variation of geometric and mechanical properties of bamboo may inform efforts underway (Trujillo 2013) to establish

methods for grading bamboo culms. It is hypothesized that due to the similarity of bamboo load demands while growing, consistent relationships between sectional and longitudinal geometry should exist that could be exploited in a grading protocol. Additionally, the inherent stiffening effect of the functionally-graded nature of the bamboo (both in section and longitudinally) may be exploited to provide greater confidence in a grading scheme based on geometry and minimal material property sampling. Similarly, a method for better modelling bamboo structures – in particular the shape finding necessary for the application of gridshells – requires an approach to modelling the tapered geometry of bamboo.

Both of these applications require geometric study of the entire culm height as it grows rather than from the relatively short culms used as compression elements described in this work. The *in situ* growing loads – predominantly from wind – are the environmental stressors under which the bamboo forms and the eventual geometric relationships between culm diameter, wall thickness, length, taper and internode length determined. Practical gridshells, too, will utilise the greatest length of the full culm as possible. Thus the approach presented in this study may be extended from the investigation of 'structural members' presented here, to the study of the full culm as it grows. Finally, it must be acknowledged that there is a great deal of variation between bamboo species in terms of geometry and material properties. A consistent approach to these issues, applied to various species – perhaps with some broad classifications such as thin- and thick-walled – is necessary to validate the trends illustrated in this work. Through such study, bamboo may be may become established as a conventional structural material.

Acknowledgements

The authors would like to gratefully acknowledge Ms. Mutsuko Grant at the Natural Materials and Structures research group at the University of Cambridge for her translation of Shigematsu (1958). The second author was supported by a Swanson School of Engineering Summer Research Internship. The third author was supported as an NSF IGERT Fellowship (NSF DGE 0504345). All work was supported by and conducted in the Watkins Haggart Structural Engineering Laboratory at the University of Pittsburgh.

References

Amada, S., Munekata, T., Nagase, Y., Ichikawa, Y., Kirigai, A. and Zhifei, Y. (1996) The mechanical structures of bamboos in viewpoint of functionally gradient and composite materials, *Journal of Composite Materials*, **30**, 800-819.

Amada, S., Ichikawa, T., Munekata, T., Nagase, Y., and Shimizu, H., (1997) Fiber texture and mechanical graded structure of bamboo, *Composites: Part B*, **28B**, 13-20.

Bumstead, J. and Harries, K.A. (2016) Effect of Variation of Geometric Properties on Bamboo Culm Buckling*, Ingenium: Undergraduate Research at the Swanson School of Engineering*, Spring 2016.

Correal, J.F. and Ardelaez, J. (2010) Influence of age and height position on Colombian *guadua angustifolia* bamboo mechanical properties*, Maderas Ciencia yTechnogia*, **12**(2), 105-113.

Dixon, P.G. and Gibson, L.J. (2014) The structure and mechanics of Moso bamboo material, *Journal of the Royal Society Interface* **11**: 20140321.

Douthe, C., Baverel, O., Caron, J.F.,(2006) Form-finding of a grid shell in composite materials, *Journal of the International Association for Shell and Spatial structures*, **47**(1), 53-62.

Duff, C.H. (1941) Bamboo and its structural uses, *The Engineering Society of China*, session 1940-41, paper #ICE-1. Institution of Civil Engineers of Shanghai, 1-27.

Eells, P., Pagliassotti, M., Brown, K., Nites, M., Stein, A., Zimmerman, C., Richard, M., Sharma, B. and Harries, K.A. (2013) Design of a Rapidly Deployable Bamboo Gridshell Structure, *14th International Conference Non-conventional Materials and Technologies* (IC-NOCMAT 2013), João Pessoa, Brazil. March 2013.

Gere. J.M and Crater, W.O. (1962) Critical Buckling Loads for Tapered Columns, *Journal of the Structural Division*, **ST1**, 3045, American Society of civil Engineers.

Ghavami, K., (2008) Bamboo: Low cost and energy saving construction materials. *Modern Bamboo Structures*, Xiao, Y., Inoue, M., and Paudel S.K., eds., London, UK, 5-21.

Ghavami K, Rodriques CS, Paciornik S (2003) Bamboo: functionally graded composite material. *Asian J. Civ. Eng. (Build Hous.)* **4**(1),1–10

Habibi, M.K., Samaei, A.T., Gheshlaghi, B., Lu, J. and Lu, Y. (2015) Asymmetric flexural behaviour from bamboo's functionally graded hierarchical structure: Underlying mechanisms, *Acta Biomaterialia*, **16**, 178-186.

International Organization for Standardization (ISO) (2004), *ISO 22157-1:2004(E), Bamboo – Determination of Physical and Mechanical Properties – Part I: Requirements*. Geneva, 2004.

Janssen, J., (1981). Bamboo in Building Structures. *Doctoral Thesis*. Eindhoven University of Technology, Netherlands.

Janssen, J.J.A., (2000). Designing and Building with Bamboo: *INBAR Technical Report 20*. International Network for Bamboo and Rattan, Beijing, China, 211pp.

Kamruzzaman, M., Saha, S.K., Bose, A.K. and Islam, M.N. (2008) Effects of Age and Height on Physical and Mechanical Properties of Bamboo, *Journal of Tropical Forests Science*, **20**(3), 211-217.

Nogata, F. and Takahashi, H. (1995) Intelligent functionally graded material: bamboo, *Composites Engineering*, **5**, 743-751.

Nugroho, N. and Bahtiar, E.T. (2013) Bamboo taper Effect on Third Point Loading Bending Test, *International Journal of Engineering and Technology*, **5**(3), 2379-2384.

Li, X.B., Shupe, T.F., Peter, G.F., Hse, C.Y., and Eberhardt, T.L., (2007). Chemical Changes with Maturation of the Bamboo Species *Phyllostachys Pubescens*. *Journal of Tropical Forest Science*, 19(1), pp. 6-12.

Li, H. and Shen S., (2011). The mechanical properties of bamboo and vascular bundles. *Journal of Materials Research*, **26**(21), 2749-2756.

Liese, W., (1987). Research on Bamboo. *Wood Science and Technology* **21**, 189-209.

Qi, J.Q., Xie, J.L., Huang, X.Y., Yu, W.J. and Chen, S.M. (2014) Influence of characteristic inhomogeneity of bamboo culm on mechanical properties of bamboo plywood: effect of culm height, *Journal of Wood Science*, **60**, 396-402.

Richard M.J. (2013) Assessing the performance of bamboo structural components, *PhD Dissertation*, University of Pittsburgh, p 288

Richard, M.J. and Harries, K.A. (2015) On Inherent Bending in Tension Tests of Bamboo, *Wood Science and Technology* **49**(1), 99-119.

Shigematsu, Y. (1958) Analytical Investigation of the Stem Form of the Important Species of Bamboo, *Bulletin of the Faculty of Agriculture*, University of Miyazaki **3,** 124-135. (in Japanese)

Southwell, E. V. (1932), On the analysis of experimental observations in problems of elastic stability, *Proceedings of Royal Society of London*, **135**, 601-616.

Trujillo, D. (2013) Prospects for a method to infer non-destructively the strength of bamboo: a research proposal, *Proceedings of the Third International Conference on Sustainable Construction Materials and Technologies*. 18-21 Aug 2013, Kyoto, Japan

Vaessen, M.J. and Janssen, J.A. (1997) Analysis of the critical length of culms of bamboo in four-point bending tests, *HERON*, **42**(2), 113-124.

Williams, F.W. and Aston, G. (1989) Exact or Lower Bound Tapered Column Buckling Loads, *ASCE Journal of Structural Engineering* **115**(5), 1088-1100.

Yu, W.K., Chung, K.F. and Chan, S.L. (2003) Column Buckling of Structural Bamboo, *Engineering Structures* **25**, 755-768.

Table 1 Effect of material property gradient on effective culm geometric properties.

E_f/E_m	D_n/t_n	$k = 0.5$[b]			$k = 1.0$[c]			$k = 2.0$[d]		
		I_{eff}/I_n	r_{eff}/r_n	t_c/t_n	I_{eff}/I_n	r_{eff}/r_n	t_c/t_n	I_{eff}/I_n	r_{eff}/r_n	t_c/t_n
10.0	4.0	1.13	1.03	0.58	1.16	1.05	0.61	1.19	1.06	0.63
	10.0	1.06	1.01		1.06	1.02		1.05	1.02	
19.4[a]	4.0	1.14	1.04	0.59	1.19	1.05	0.62	1.22	1.07	0.65
	10.0	1.06	1.01		1.07	1.02		1.06	1.03	
30.0	4.0	1.15	1.04	0.59	1.20	1.07	0.63	1.23	1.08	0.66
	10.0	1.06	1.02		1.07	1.02		1.07	1.03	

[a] Janssen (1981, 2000)
[b] similar to $k = 0.43$ reported by Habibi et al. (2015)
[c] Duff (1941), Janssen (1981, 2000) and Vaessen and Janssen (1997)
[d] Ghavami et al. (2003) and similar to $k \approx 2.2$ reported by Nogata and Takahashi (1995)

Table 2 Trends of measured (D and t) and calculated (A, I and r) geometric properties along the normalised culm length.

	P. edulis (Moso)	*B. stenostachya* (Tre Gai)	*G. angustifolia* (Guadua)
number of samples	10 culms 116 measurements	19 culms 222 measurements	14 culms 163 measurements
D/t	average = 10.3 COV = 0.17 minimum = 5.9 maximum = 13.4	average = 5.5 COV = 0.22 minimum = 3.1 maximum = 8.4	average = 11.5 COV = 0.18 minimum = 6.3 maximum = 18.4
$ln(D/D_0)$ =	-0.007(L/D_0) R^2 = 0.85	-0.0006(L/D_0) R^2 = 0.01	-0.003(L/D_0) R^2 = 0.47
$ln(t/t_0)$ =	-0.019(L/D_0) R^2 = 0.36	-0.017(L/D_0) R^2 = 0.82	-0.009(L/D_0) R^2 = 0.02
$ln(A/A_0)$ =	-0.024(L/D_0) R^2 = 0.60	-0.014(L/D_0) R^2 = 0.79	-0.012(L/D_0) R^2 = 0.27
$ln(I/I_0)$ =	-0.036(L/D_0) R^2 = 0.80	-0.009(L/D_0) R^2 = 0.45	-0.017(L/D_0) R^2 = 0.71
$ln(r/r_0)$ =	-0.006(L/D_0) R^2 = 0.76	0.0022(L/D_0) R^2 = 0.32	-0.003(L/D_0) R^2 = 0.26

Table 3 Culm buckling analyses conducted.

Case	Description	*P. edulis* (Moso)	*B. stenostachya* (Tre Gai)	*G. angustifolia* (Guadua)
I	prismatic culm using properties at culm base	D_0 = 100 mm; t_0 = 10 mm A_0 = 2827 mm^2 I_0 = 2,898,119 mm^4 E_0 = 15080 MPa	D_0 = 100 mm; t_0 = 25 mm A_0 = 5890 mm^2 I_0 = 4,601,942 mm^4 E_0 = 15080 MPa	D_0 = 100 mm; t_0 = 9 mm A_0 = 2573 mm^2 I_0 = 2,689,391 mm^4 E_0 = 15080 MPa
II	prismatic culm using properties at top of 2500 mm culm (L/D_0 = 25)	$A_T = A_0e^{-0.024(25)}$ = 1552 mm^2 $I_T = I_0e^{-0.036(25)}$ = 1,178,287 mm^4 E_0 = 15080 MPa	$A_T = A_0e^{-0.014(25)}$ = 4151 mm^2 $I_T = I_0e^{-0.009(25)}$ = 3,674,726 mm^4 E_0 = 15080 MPa	$A_T = A_0e^{-0.012(25)}$ = 1906 mm^2 $I_T = I_0e^{-0.017(25)}$ = 1,758,243 mm^4 E_0 = 15080 MPa
III	prismatic culm having average properties of base and top	A = 2190 mm^2 I = 2,038,203 mm^4 E_0 = 15080 MPa	A = 5021 mm^2 I = 4,138,334 mm^4 E_0 = 15080 MPa	A = 2239 mm^2 I = 2,223,817 mm^4 E_0 = 15080 MPa
IV	prismatic culm having properties calculated at midheight	$A_T = A_0e^{-0.024(12.5)}$ = 2095 mm^2 $I_T = I_0e^{-0.036(12.5)}$ = 1,847,922 mm^4 E_0 = 15080 MPa	$A_T = A_0e^{-0.014(12.5)}$ = 4945 mm^2 $I_T = I_0e^{-0.009(12.5)}$ = 4,112,283 mm^4 E_0 = 15080 MPa	$A_T = A_0e^{-0.012(12.5)}$ = 2215 mm^2 $I_T = I_0e^{-0.017(12.5)}$ = 2,174,535 mm^4 E_0 = 15080 MPa
V	linear taper of geometric properties from bottom to top	$A = A_0 - (A_0\text{-}A_T)(x/L)$ $I = I_0 - (I_0\text{-}I_T)(x/L)$ E_0 = 15080 MPa	$A = A_0 - (A_0\text{-}A_T)(x/L)$ $I = I_0 - (I_0\text{-}I_T)(x/L)$ E_0 = 15080 MPa	$A = A_0 - (A_0\text{-}A_T)(x/L)$ $I = I_0 - (I_0\text{-}I_T)(x/L)$ E_0 = 15080 MPa
VI	tapered geometry (Table 2)	$A = A_0e^{-0.024(x/D0)}$ $I = I_0e^{-0.036(x/D0)}$ E_0 = 15080 MPa	$A = A_0e^{-0.014(x/D0)}$ $I = I_0e^{-0.009(x/D0)}$ E_0 = 15080 MPa	$A = A_0e^{-0.012(x/D0)}$ $I = I_0e^{-0.017(x/D0)}$ E_0 = 15080 MPa
VII	tapered geometry (Table 2) and 10% linear increase of modulus	$A = A_0e^{-0.024(x/D0)}$ $I = I_0e^{-0.036(x/D0)}$ $E = E_0(1 + 0.1x/L)$	$A = A_0e^{-0.014(x/D0)}$ $I = I_0e^{-0.009(x/D0)}$ $E = E_0(1 + 0.1x/L)$	$A = A_0e^{-0.012(x/D0)}$ $I = I_0e^{-0.017(x/D0)}$ $E = E_0(1 + 0.1x/L)$
VIII	tapered geometry (Table 2) and 20% linear increase of modulus	$A = A_0e^{-0.024(x/D0)}$ $I = I_0e^{-0.036(x/D0)}$ $E = E_0(1 + 0.2x/L)$	$A = A_0e^{-0.014(x/D0)}$ $I = I_0e^{-0.009(x/D0)}$ $E = E_0(1 + 0.2x/L)$	$A = A_0e^{-0.012(x/D0)}$ $I = I_0e^{-0.017(x/D0)}$ $E = E_0(1 + 0.2x/L)$

Table 4 Result of buckling analysis of pin-ended culms.

Case	*P. edulis* (Moso)				*B. stenostachya* (Tre Gai)				*G. angustifolia* (Guadua)			
	P_{cr}	$P_{cr}/P_{cr,II}$	$f_{cr} = P_{cr}/A_T$	$h_{\Delta max}$[a]	P_{cr}	$P_{cr}/P_{cr,II}$	$f_{cr} = P_{cr}/A_T$	$h_{\Delta max}$[a]	P_{cr}	$P_{cr}/P_{cr,II}$	$f_{cr} = P_{cr}/A_T$	$h_{\Delta max}$[a]
	kN		MPa	1/L	kN		MPa	1/L	kN		MPa	1/L
I	69.1	2.46	44.6	0.50	109.8	1.25	26.4	0.50	64.2	1.53	33.7	0.50
II	28.1	1.00	18.1	0.50	87.7	1.00	21.1	0.50	41.9	1.00	22.0	0.50
III	48.6	1.73	31.3	0.50	98.7	1.13	23.8	0.50	53.1	1.26	27.8	0.50
IV	44.1	1.57	28.4	0.50	98.1	1.12	23.6	0.50	51.9	1.24	27.2	0.50
V	46.6	1.66	30.1	0.54	98.3	1.12	23.7	0.50	52.4	1.25	27.5	0.52
VI	42.7	1.52	27.5	0.54	97.7	1.11	23.5	0.50	51.4	1.23	27.0	0.52
VII	45.1	1.61	29.1	0.52	102.8	1.17	24.8	0.50	54.1	1.29	28.4	0.52
VIII	47.4	1.69	30.6	0.52	107.8	1.23	26.0	0.50	56.8	1.35	29.8	0.50

[a] height along culm corresponding to maximum lateral displacement measured from base

Table 5 Buckling analyses of experimental test results.

		P. edulis (Moso)				*B. stenostachya* (Tre Gai)			
		Culm 1	Culm 2	Culm 3	Culm 4	Culm 5	Culm 6	Culm 7	Culm 8
E	MPa	6645 (COV = 0.08)				13,450 (COV = 0.32)			
KL	mm	2410	2420	2410	2290	2600	2600	1942	2210
out-of-straightness		L/172	L/100	L/142	L/208	L/113	L/200	L/235	L/153
internodes		11	10	8	9	12	15	12	13
D_0	mm	111.1	106.7	75.4	89.5	86.1	88.0	89.2	85.3
t_0	mm	11.0	13.2	6.5	7.9	18.4	20.2	22.0	21.1
A_0	mm^2	3456	3890	1410	2036	3920	4303	4641	4250
I_0	mm^4	4,384,070	4,334,547	843,942	1,710,633	2,413,455	2,696,455	2,903,574	2,428,630
D_{top}	mm	100.0	93.3	58.7	67.1	91.0	90.3	87.9	87.2
t_{top}	mm	8.0	8.2	5.8	6.4	11.6	10.7	12.9	12.0
A_{top}	mm^2	2318	2193	964	1224	2889	2675	3043	2844
I_{top}	mm^4	2,471,053	2,005,633	341,845	569,169	2,324,157	2,157,478	2,203,771	2,061,868
average A	mm^2	2887	3041	1187	1630	3404	3489	3842	3547
average I	mm^4	3,427,561	3,170,090	592,893	1,139,901	2,368,806	2,426,966	2,553,672	2,245,249
A at $L/2$	mm^2	2670	2616	1233	1610	3263	3082	3744	3500
I at $L/2$	mm^4	3,152,014	2,638,391	631,183	1,057,774	2,433,920	2,049,207	2,550,298	2,240,170
		critical buckling load (ratio of predicted/experimental)							
experimental	kN	44.6	38.8	9.3	18.8	52.3	49.9	95.7	62.6
Case I	kN	49.6 (1.11)	48.7 (1.26)	9.5 (1.02)	21.4 (1.14)	47.4 (0.91)	53.0 (1.06)	102.4 (1.07)	66.1 (1.06)
Case II	kN	28.0 (0.63)	22.5 (0.58)	3.9 (0.42)	7.1 (0.38)	45.7 (0.87)	42.4 (0.85)	77.7 (0.71)	56.1 (0.89)
Case III	kN	38.8 (0.87)	35.6 (0.92)	6.7 (0.72)	14.3 (0.76)	46.5 (0.89)	47.7 (0.96)	90.1 (0.94)	61.1 (0.98)
Case IV	kN	35.7 (0.80)	29.6 (0.76)	7.1 (0.76)	13.2 (0.70)	47.9 (0.92)	40.3 (0.81)	90.0 (0.94)	61.0 (0.97)
Case VI	kN	37.8 (0.85)	30.7 (0.79)	8.5 (0.91)	13.0 (0.69)	47.5 (0.91)	42.0 (0.84)	85.2 (0.89)	59.6 (0.95)

Table 6 Characteristics of thin- and thick-walled bamboo species.

	Thin-walled	Thick-walled
represented by	*P. edulis* (Moso) *G. angustifolia* (Guadua)	*B. stenostachya* (Tre Gai)
D/t	> 8	< 8
radius of gyration, *r*	decreases with height	increased with height
effect of material property gradient on effective culm geometric properties (see Table 1)	marginal, less than 5% increase	10-20% increase
increase in buckling capacity over that calculated using minimal section (see Table 4)	significant: Moso greater than 50% Guadua greater than 25%	marginal, less than 12%

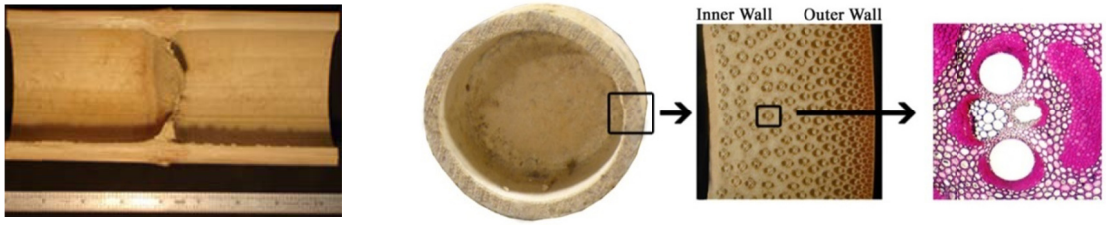

a) longitudinal section of bamboo culm showing portions of internodes to either side of node

b) cross section of culm near node diaphragm

c) section through culm wall

d) vascular bundle (vessels (white) and fibers (dark) embedded in lignin matrix)

Figure 1 Anatomy of bamboo culm (adapted from Richard 2013).

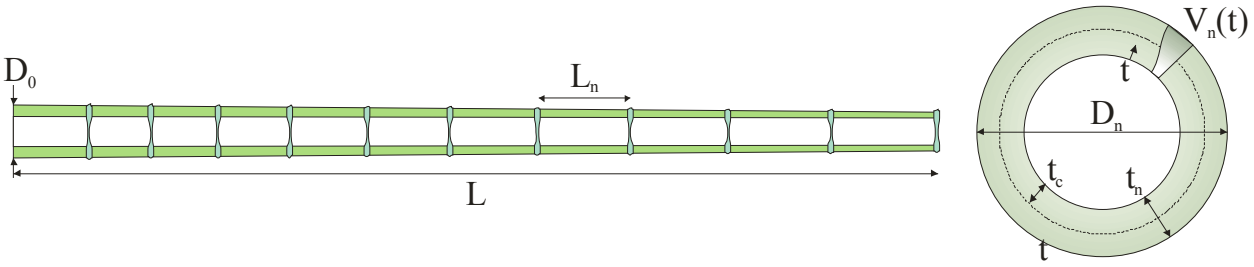

Figure 2 Measured culm properties.

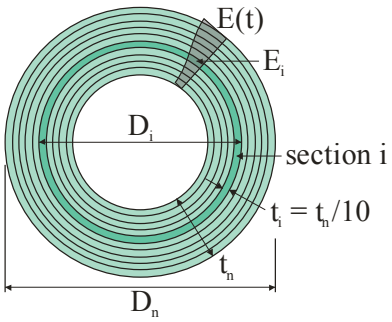

Figure 3 Discretisation of culm section.

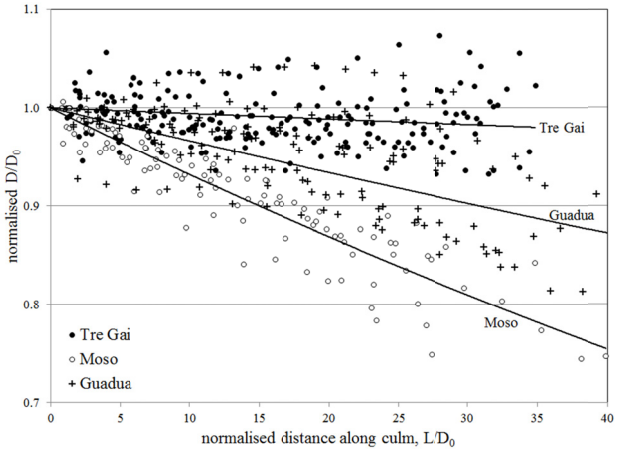

a) variation of normalised culm diameter (D/D_0)

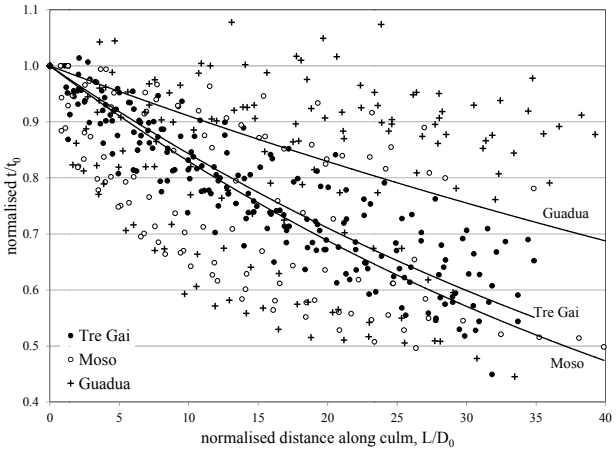

b) variation of normalised culm wall thickness (t/t_0)

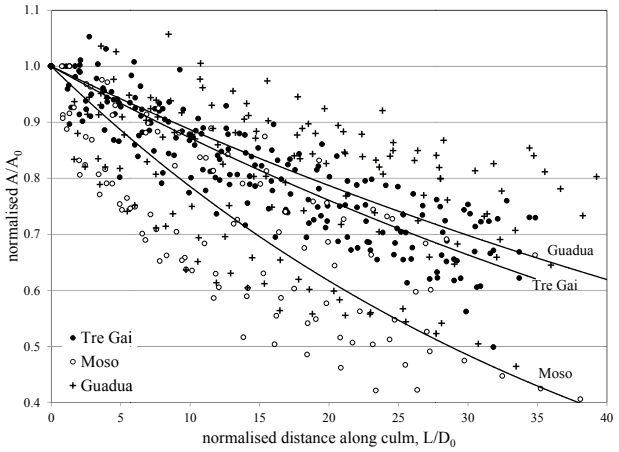

c) variation of normalised culm cross sectional area (A/A_0)

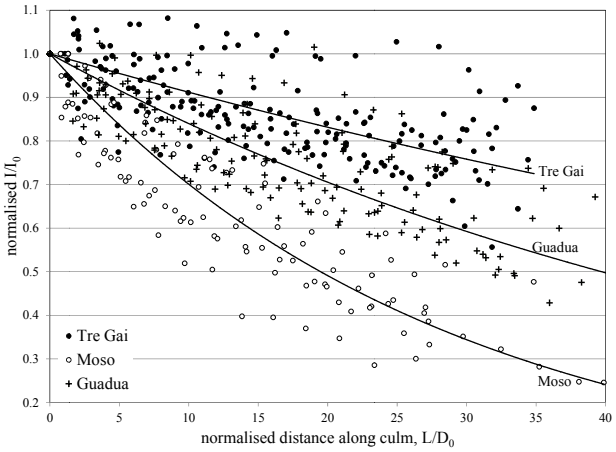

d) variation of normalised culm cross sectional moment of inertia (I/I_0)

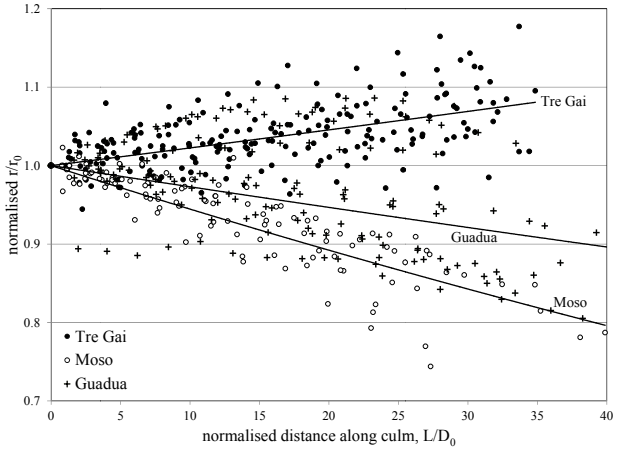

e) variation of normalised culm radius of gyration (r/r_0)

Figure 4 Variation of normalised geometric properties with culm length.

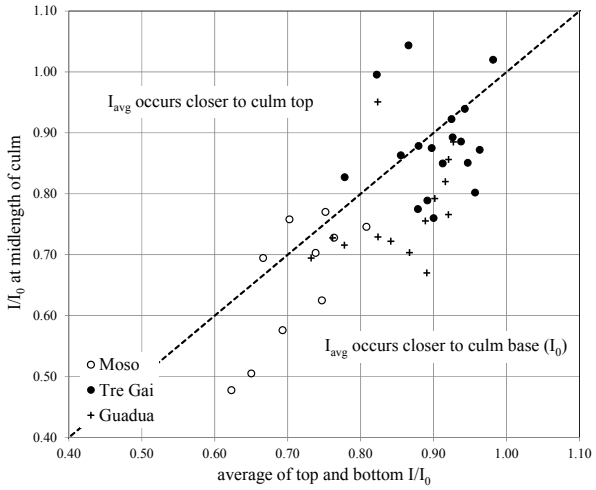

Figure 5 Measured moment of inertia at culm midheight versus average moment of inertia calculated from base and top values.

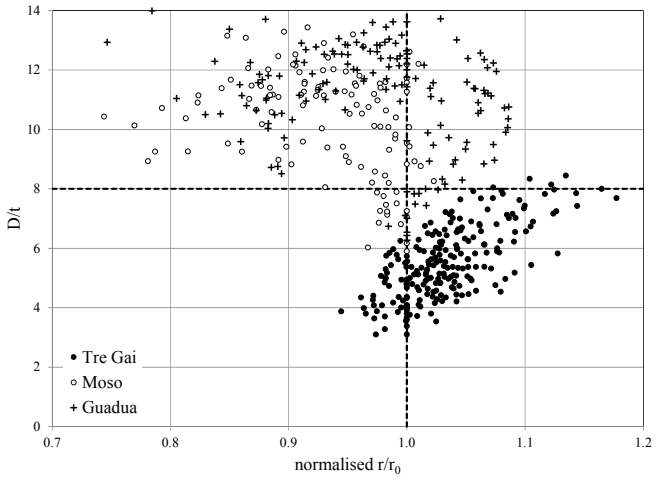

Figure 6 Classification of culm by variation of radius of gyration.